IEEE Access
Multidisciplinary | Rapid Review | Open Access Journal

Received August 30, 2018, accepted September 19, 2018, date of publication October 4, 2018, date of current version October 29, 2018.

Digital Object Identifier 10.1109/ACCESS.2018.2873572

PMU-Based Estimation of Synchronous Machines' Unknown Inputs Using a Nonlinear Extended Recursive Three-Step Smoother

JAN LAVENIUS[1], (Student Member, IEEE), AND LUIGI VANFRETTI[2], (Senior Member, IEEE)
[1]Department of Electric Power and Energy Systems, KTH Royal Institute of Technology, 100 44 Stockholm, Sweden
[2]Department of Electrical, Computer, and Systems Engineering, Rensselaer Polytechnic Institute, Troy, NY 12180, USA

Corresponding author: Jan Lavenius (janlav@kth.se)

The work of J. Lavenius was supported in part by Statnett SF, the Norwegian TSO, through the RT VS Project. The work of L. Vanfretti was supported in part by the Engineering Research Center Program of the National Science Foundation, in part by the Department of Energy under Award EEC-1041877, and in part by the CURENT Industry Partnership Program.

ABSTRACT Knowledge of the synchronous machines' control input signals and internal states can provide valuable insight to system operators for assessing security margins and the stability of the power system. For example, during disturbances in a stressed power system, it can be of great value to monitor the performance of the machine's control system, e.g., the response of the field voltage, mechanical power, and the field current. As there are often no real-time power plant measurements available to power system operators, internal states, and unknown inputs of generator units would need to be estimated from synchrophasor measurements. This paper proposes a new estimation algorithm, the nonlinear extended recursive three-step smoother (NERTSS), to simultaneously estimate the states and the unknown inputs of the synchronous machine using data from phasor measurement units. These quantities can then be used to monitor the performance of the machine's controls. The case studies presented in the paper compare the estimation performance of the NERTSS with the extended Kalman filter with unknown inputs (EKF-UI) when noisy synchrophasor measurements are used. The simulation results show that the proposed estimation method compares favorably with respect to the EKF-UI in terms of the achieved estimation accuracy.

INDEX TERMS Synchronous generator, Kalman filters, phasor measurement units, power system operation, state estimation, unknown input estimation.

I. INTRODUCTION

A. MOTIVATION

The task of operating a transmission system includes ensuring that the electrical network remains within its required operational limits and that it is stable even under disturbances. The monitoring of the system, as carried out by transmission system operators, traditionally uses supervisory control and data acquisition (SCADA) systems to acquire data and reconstruct the voltages and power flows of the grid for a single snapshot over a pre-defined time-window. However, the snapshots provided by a SCADA system are taken asynchronously in a time-scale from seconds to minutes. This means that dynamic events that evolve between SCADA snapshots cannot be accurately captured and presented to operators. Time-synchronized phasor data provided by phasor measurement units (PMUs) can provide the temporal resolution needed to capture these dynamic events. There also may exist a need to estimate quantities that lie outside the transmission system itself to ensure the stability of the entire grid. For example, the states and inputs of synchronous machines are of importance when considering a power system's stability. In [1], it is shown that a power systems can a undergo voltage collapse that is precipitated by the enforcement of over-excitation limits of synchronous machines. Therefore, a good estimate of the time remaining before the over-excitation limiter becomes active could be used as a constraint for the corrective actions that can be applied after a contingency. In this case, the field voltage and field current estimates would need to be calculated from PMU data using state and input estimation methods due to the unavailability of real-time power plant measurements to the operator. Tracking the unknown inputs can also be used to monitor the controller performance of the machine's turbine governor and excitation system.

B. LITERATURE REVIEW

Much research has been devoted to the possibility to use synchrophasor measurements, that is synchronized data obtained from PMUs, for estimating the state of the power system between SCADA snapshots. The scope of this paper is the state and input estimation of synchronous machines and this literature review is therefore focused on this subject.

Reference [2] used neural networks to estimate the internal states of the machines. Mandal *et al.* [3] proposed the extended Kalman filter (EKF) to solve dynamic state estimation problems in power systems. In [4], Ghahremani and Kamwa proposed an EKF to estimate the internal states of synchronous machines, which in the same paper was combined with a simultaneous estimation of the unknown inputs as the extended Kalman filter with unknown inputs (EKF-UI). The estimation model in the original EKF-UI formulation was only valid when connected to an infinite bus. The EKF-UI was therefore further developed in [5] with an augmented state vector such that the internal machine angle could be estimated from terminal quantities. It is known [6], [7] that the EKF can suffer performance degradation if the Jacobian matrices used for linearization are sensitive to errors in the state estimates or other inputs. An alternative approach using statistical linearization was used by the unscented Kalman filter (UKF) in [8], which was further developed in [9] for the estimation of the unknown inputs as an unscented Kalman filter with unknown inputs (UKF-UI). Reference [9] also investigated a cubature Kalman filter with unknown inputs (CKF-UI), which requires less tuning than the UKF-UI. Reference [10] used a particle filter to enhance the accuracy when estimating the states but this approach requires additional computational time compared to UKF and is also dependent on the measurement of the mechanical power. Reference [11] provides a comparative study of synchronous machine state estimation algorithms, but the study is limited to state estimation only, i.e. it does not consider unknown inputs.

In the automatic control community much research has been devoted to minimum variance state estimation of systems without feed-through of the unknown inputs, starting with the Kitanidis filter in [12] and later by the descriptor Kalman filter in [13]. The general, linear discrete-time case was solved in [14] using an innovations approach to derive optimal filters for an equivalent unknown input-decoupled system. The extended recursive three-step filter (ERTSF) of [15] combined the unknown input-decoupling with unknown input estimation, which was then adapted to nonlinear systems in [16] as the nonlinear extended recursive three-step filter (NERTSF).

This paper proposes a new method to simultaneously estimate unknown inputs and non-linear states, in which the nonlinear estimation of the NERTSF is combined with the smoothing algorithm of [17], to achieve better estimates of states and unknown inputs.

C. CONTRIBUTIONS OF THIS PAPER

The main contributions of this paper are the following,

(i) A new estimation method, the nonlinear extended recursive three-step smoother (NERTSS), and a new, alternative estimation model for the purpose of simultaneously estimating the states and unknown inputs of synchronous machines.
(ii) The use of Monte Carlo simulations to investigate the performance of the EKF-UI and the NERTSS algorithms to synchronous machine' state and unknown input estimation using noisy synchrophasor measurements.
(iii) Proposing potential applications of simultaneous state and unknown input estimation for real-time control system performance monitoring.

The remainder of this paper is organized as follows, Section II details the estimation algorithms including the new NERTSS method proposed in this paper, in Section III the estimation models for the considered synchronous machine are presented, Section IV details the noise modeling used by the numerical experiments conducted in Section V, Section VI discusses the computational performance and gives example of possible practical applications. Finally, Section VII summarizes the main conclusions from this work.

II. METHODS FOR UNKNOWN INPUT AND STATE ESTIMATION

For estimation purposes, it is convenient to use state-space models that are formulated in discrete time. A simple method of transforming continuous time models to discrete time is by applying Euler's forward method, in whichthe state equations $f(x(t), d(t), u(t))$ and the output equations $g(x(t), d(t), u(t))$ are sampled with a small sampling time T_s, giving a discrete-time state-space representation

$$x_{k+1} = f_k(x_k, d_k, u_k) + w_k, \tag{1}$$
$$y_k = g_k(x_k, d_k, u_k) + v_k, \tag{2}$$

where the process noise w_k and the measurement noise v_k were both assumed to be additive. The noise sequences w_k and v_k are both assumed to be uncorrelated, zero-mean and white sequences and having the covariance matrices $Q_k \geq 0$, $R_k \geq 0$, respectively.

A. THE EXTENDED KALMAN FILTER WITH UNKNOWN INPUTS (EKF-UI)

The idea behind the EKF is that the evolution of a nonlinear system can be approximately described by a linear time-varying system obtained by successive linearization around the current state estimate $\hat{x}_{k|k}$ at time instant k. For compactness of notation, the explicit conditioning of variables, e.g. $k|k$ in the subscripts, is omitted when the conditioning is obvious from the context. For the classical EKF, an approximate estimator for the state x_k is recursively given by the

calculation of (3)-(7) at each time instant k:

$$\hat{x}_{k+1|k} = f_k(\hat{x}_{k|k}, u_k), \tag{3}$$
$$\hat{x}_{k|k} = \hat{x}_{k|k-1} + K_k\left[y_k - g_k(\hat{x}_{k|k-1}, u_k)\right], \tag{4}$$
$$K_k = P_{k|k-1}C_k^T\left(C_kP_{k|k-1}C_k^T + R_k\right)^{-1}, \tag{5}$$
$$P_{k|k} = (I - K_kC_k)\,P_{k|k-1}, \tag{6}$$
$$P_{k+1|k} = A_kP_{k|k}A_k^T + Q_k, \tag{7}$$

where K_i is the Kalman gain and where A_k, C_k are, respectively, the following matrices of partial derivatives:

$$A_k = \frac{\partial f_k(x_k, u_k)}{\partial x}|_{x_k=\hat{x}_{k|k}}, \tag{8}$$
$$C_k = \frac{\partial g_k(x_k, u_k)}{\partial x}|_{x_k=\hat{x}_{k|k-1}}. \tag{9}$$

The EKF described by (3)-(7) assumes that: 1) only the states x_k and noise (v_k, w_k) are unknown; 2) the functions f_k and g_k are known; and 3) the partial derivative matrices (8), (9) can be obtained exactly or approximated numerically. In synchronous machine applications, these three assumptions may fail to hold. For example, some elements of the input vector u_k, e.g. the bus voltage magnitude V_t, influence the state function $f_k(x_k, u_k)$, but may only be available as noisy measurements. Furthermore, the mechanical power P_m and the field voltage E_{fd} are typically not available outside the power plant and have to be estimated. Using the algorithm proposed in [18], an EKF-UI for synchronous machines was proposed in [4]. It should be noted that the variety of EKF-UI used in [4] assumes no direct feed-through of unknown inputs as stated in [19]. For comparative purposes, this paper uses the EKF-UI algorithm as given in [19]. The elements of the input vector u_k in (3)-(9) that are not known will in the following be denoted by d_k. In the EKF-UI, the unknown inputs d_{k-1} and the states x_k are estimated recursively at time instant k using (3)-(5), (7)-(9) and

$$S_k = \left[G_{k-1}^TC_k^TR_k^{-1}\left(I - C_kK_i\right)C_kG_{k-1}\right]^{-1}, \tag{10}$$
$$\hat{u}^*_{k-1|k} = S_kG_{k-1}^TC_k^TR_k^{-1}\left(I - C_kK_i\right) \times\left(y_k - g_k(\hat{x}_{k|k-1}, u_k) + C_kG_{k-1}\hat{u}^*_{k-2|k-1}\right), \tag{11}$$
$$P_{k|k} = (I - K_kC_k)\left(P_{k|k-1} + G_{k-1}S_kG_{k-1}^T\left(I - K_kC_k\right)^T\right), \tag{12}$$

where G_{k-1} is the matrix of partial derivatives of the state equation $f_k(\cdot)$ with respect to the unknown inputs d_{k-1} given by

$$G_{k-1} = \frac{\partial f_k(x_k, d_k, u_{k-1})}{\partial d_k}|_{x_k=\hat{x}_{k-1|k-1}, d_k=\hat{d}_{k-2|k-1}}, \tag{13}$$

at time $k-1$. Because there is no direct feed-through, $\hat{d}_{k-1|k-2}$ will be used for the linearization in (13).

B. THE NONLINEAR EXTENDED RECURSIVE THREE-STEP FILTER (NERTSF)

NERTSF was proposed in [16] as a non-linear extension of the filtering algorithm of [15] and assumes that there is no direct feed-through between the unknown inputs and the outputs. In contrast to the EKF-UI, the NERTSF performs the unknown input and state estimation in the reverse order, by first estimating the unknown inputs d_{k-1} before estimating the state x_k. The three steps of the NERTSF algorithm are summarized in the remainder of this subsection and the reader is referred to [16] for a more detailed exposition:

Step 1: Time update at time instant k:

$$\hat{x}_{k|k-1} = f(\hat{x}_{k-1|k-1}, \hat{d}_{k-1|k-1}, u_{k-1}), \tag{14}$$
$$P^x_{k|k-1} = A_{k-1}P^x_{k-1|k-1}A_{k-1} + Q_{k-1}, \tag{15}$$

where A_k is given in (8) and $P^x_{k|k}$ is the state error covariance at time k and the unknown input distribution matrix G_{k-1} is given by (13).

Step 2: Generate the decoupling unknown input estimate:

$$\tilde{R}_k = C_kP^x_{k|k-1}C_k^T + R_k, \tag{16}$$
$$S_k = C_kG_{k-1}, \tag{17}$$
$$P^{\hat{d}}_{k|k} = (S_k^T(\tilde{R}_k)^{-1}S_k)^{-1}, \tag{18}$$
$$M_k = (S_k^T\tilde{R}_k^{-1}S_k)^{-1}S_k^T\tilde{R}_k^{-1}, \tag{19}$$
$$\hat{d}_{k-1|k} = M_k\left(y_k - g(\hat{x}_{k|k-1}, \hat{d}_{k-1|k-1}, u_k)\right), \tag{20}$$

where C_k is given by (9) and G_{k-1} by (13). After performing Step 2, the a-priori predictions in (14), (15) are updated using the substitution $\hat{d}_{k-1|k-1} \leftarrow \hat{d}_{k|k}$, because the state and output equations may be highly non-linear.

Step 3: Estimate the unknown input-decoupled states:

$$K_k = P^x_{k|k-1}C_k^T\tilde{R}_k^{-1}, \tag{21}$$
$$L_k = K_k + (I_n - K_kC_k)G_{k-1}M_k, \tag{22}$$
$$\Psi_k = \tilde{R}_k(L_k - K_k)^T, \tag{23}$$
$$\hat{x}_{k|k} = \hat{x}_{k|k-1} - L_k\left(y_k - g(\hat{x}_{k|k-1}, \hat{d}_{k-1|k}, u_k)\right), \tag{24}$$
$$P^x_{k|k} = P^x_{k|k-1} - L_k\tilde{R}_kL_k^T - L_k\Psi_k + (L_k\Psi_k)^T, \tag{25}$$
$$P^{xd}_k = -P^x_{k-1|k-1}A_{k-1}^TC_k^TM_k^T. \tag{26}$$

The equations (14)-(26) define the NERTSF recursion, provided that initial estimates of the states $\hat{x}_{0|0}$, unknown inputs $\hat{d}_{0|0}$, and the initial state error covariance $P^x_{0|0}$ are given.

C. THE NONLINEAR EXTENDED RECURSIVE THREE-STEP SMOOTHER (NERTSS)

For the linear case [20], it is established that the unknown input estimate $\hat{d}_{k-1|k}$ (20) given by the ERTSF is the one-step delayed minimum variance unbiased (MVU) estimator of d_{k-1} and that the ERTSF decouples the estimated input $d_{k-1|k}$ from the estimated state $x_{k|k}$. In the non-linear case, due to the various approximations that are used to make the problem tractable, the decoupling will not be exact and no guarantees can be given about the estimator being MVU.

If the covariance matrix $P^d_{k-1|k}$ of the unknown input estimate is large then the resulting input estimate $\hat{d}_{k-1|k}$ will be uncertain. Attempting to reduce this variance, a smoothed estimate of the unknown input $\hat{d}^s_{k-1|k}$ is made by combining forward and backward filtering estimates of $\hat{d}_{k-1|k}$. The smoothed estimate thus incorporates the information gained from subsequent estimates to update an earlier estimate. Direct implementation of the backward filter would require an inversion of the dynamic equations. This can be be avoided by performing the smoothing step as a backward pass using the estimates obtained from forward filtering. State estimators that combine forward and backward passes in this way are known as Rauch-Tung-Striebel (RTS) smoothers. Using an RTS smoother for unknown input estimation was first proposed in [17], where it was named the Updated Linear Input and State Smoother (ULISS), as a further development of the estimator given in [21].

To perform state and unknown input estimation this paper proposes the NERTSS, in which the one-step smoothing backward pass from the ULISS is combined with the forward pass from the NERTSF. The NERTSS first performs a forward pass using the NERTSF algorithm (14)-(26) and then performs the backward pass of the ULISS algorithm [17]. To explain the backward pass of ULISS, the joint distribution of x_k and d_k is defined by the Gaussian distribution $\mathcal{N}\left(X_k; \hat{X}_k, P^X_k\right)$ where $P^X_k = \begin{bmatrix} P^x_k & P^{xd}_{k|N} \\ P^{dx}_k & P^d_k \end{bmatrix}$, and where $X_k = [x_k^T \;\; d_k^T]^T$. Using the same standard assumptions as for extended Kalman filtering, the joint filtering distribution $p(x_k, d_k, x_{k+1}|y_{0:k}, u_{0:k})$ is approximated by a Gaussian distribution:

$$\mathcal{N}\left(\begin{bmatrix} X_k \\ x_{k+1} \end{bmatrix}; \begin{bmatrix} \hat{X}_k \\ \hat{x}_{k+1|k} \end{bmatrix}, \begin{bmatrix} P^X_{k|k} & \bar{J}_k \\ \bar{J}_k^T & P^x_{k+1} \end{bmatrix}\right) \tag{27}$$

where $\bar{J}_k = [\bar{J}^T_{1,k} \;\; \bar{J}^T_{2,k}]^T$ with elements consisting of the covariances $\bar{J}_{1,k} = \mathrm{Cov}\,(x_k, x_{k+1})$ and $\bar{J}_{2,k} = \mathrm{Cov}\,(d_k, x_{k+1})$. Using $\bar{J}_k$ and P^x_{k+1}, the covariance of the state estimate at $k+1$, the Kalman smoother gain J_k can be obtained from the maximum likelihood of the joint filtering distribution as

$$J_k = \bar{J}_k \left(P^x_{k+1}\right)^{-1} = \begin{bmatrix} P^x_k A^T_k + P^{xd}_k G^T_k \\ P^{dx}_k A^T_k + P^d_k G^T_k \end{bmatrix} \left(P^x_{k+1}\right)^{-1} \tag{28}$$

where $P^{xd}_k = \left(P^{dx}_k\right)^T$ is given by (26). The Kalman smoother gain J_k is then used to update the mean and covariance of the filter estimates recursively, given estimates up to $N = k + L$, as:

$$\hat{X}_{k|N} = \begin{bmatrix} \hat{x}^s_k \\ \hat{d}^s_k \end{bmatrix} = \begin{bmatrix} \hat{x}_k \\ \hat{d}_k \end{bmatrix} + J_k(\hat{x}_{k+1|N} - \hat{x}_{k+1|k}) \tag{29}$$

$$P^X_{k|N} = P^X_{k|N} + J_k(\hat{x}_{k+1|N} - \hat{x}_{k+1|k})J^T_k, \tag{30}$$

where the partial derivatives and the filter means and covariances were obtained by doing a forward filtering pass of the NERTSF algorithm (14)-(26). Note that if $N = k + 1$ is chosen, then the smoothed estimate $\hat{d}^s_{k|k+1}$ will not be more delayed after the current time k than the forward-filtered estimate $\hat{d}_{k|k+1}$. Hence, a smoothing sequence of length $L = N - k = 1$ is chosen to ensure that the unknown input estimates of d_{k-1} are not delayed more than one-step, which can be a desirable property for some applications. For online estimation purposes, this paper proposes to use only the filtered state estimates $\hat{x}_{k|k}$ and not the smoothed state estimates $\hat{x}^s_{k|k}$ in order to avoid a delay when estimating the states. By allowing larger delays L, input estimates with lower variance may be obtained because the estimates would then be conditioned on more measurement points [22]. As stated above, smoothed state estimates $\hat{x}^s_{k|k+L}$ can also be obtained with this method, but they would be delayed with at least one sample since $L \geq 1$ and may therefore be of less interest for real-time applications. The proposed method will therefore, because it is targeting on-line applications, output the filtered state estimates $\hat{x}_{k|k}$ and the smoothed unknown input estimates $\hat{d}^s_{k-1|k}$ at the current time instant k.

III. SYNCHRONOUS MACHINE MODELING FOR ESTIMATION

The differential equations that describe the behavior of synchronous machines are often conveniently expressed in the *dq0*-domain by applying Park's transformation. This paper considers a fourth-order model that is formulated in the phasor domain. The principles will be valid for any machine model-order and more detailed estimation models can therefore be constructed. For the purpose of obtaining analytic Jacobians with respect to the states, the paper assumes that there is no saturation. Furthermore, the armature resistance is assumed to be negligible, $R_a \approx 0$. By denoting the machine's bus voltage phasor as $\bar{V}_t = V_t \angle \theta_{V_t}$ and the internal machine angle as $\delta_i = \delta - \theta_{V_t}$, the machine is described by the following four state equations:

$$\dot{x}_1 = \omega_0 x_2, \tag{31}$$

$$\dot{x}_2 = \frac{1}{J}\left[P_m - P_e - D x_2\right], \tag{32}$$

$$\dot{x}_3 = \frac{1}{T'_{d0}}\left[u_2 - x_3 - (x_d - x'_d)\frac{(x_3 - u_1\cos(\delta_i))}{x'_d}\right], \tag{33}$$

$$\dot{x}_4 = \frac{1}{T'_{q0}}\left[-x_4 - (x_q - x'_q)\frac{(x_4 - u_1\sin(\delta_i))}{x'_q}\right], \tag{34}$$

where x is the state vector and the u is the vector of inputs given as

$$x = \begin{bmatrix} \delta & \Delta\omega & e'_q & e'_d \end{bmatrix}^T, \tag{35}$$

$$u = \begin{bmatrix} E_{fd} & V_t & P_m \end{bmatrix}^T. \tag{36}$$

The active power P_e and the reactive power Q_e exchanged between the machine and the network are given

by

$$P_e = \frac{V_t e'_q}{x'_d}\sin\delta_i - \frac{V_t e'_d}{x'_q}\cos\delta_i + V_t^2\frac{x'_d - x'_q}{2x'_d x'_q}\sin 2\delta_i, \quad (37)$$

$$Q_e = \frac{V_t e'_d}{x'_q}\sin\delta_i + \frac{V_t e'_q}{x'_d}\cos\delta_i - V_t^2\left(\frac{\cos^2\delta_i}{x'_d} + \frac{\sin^2\delta_i}{x'_q}\right), \quad (38)$$

respectively, using the generator convention for the direction of the power flows. The state variable $\Delta\omega$ is the rotor speed deviation from nominal speed and all quantities in (31)-(38) are assumed to be on the per unit-scale, except the angles which are assumed to be in radians. Note that for salient-pole machines $e'_d = x_4 = 0$ and $x'_q = x_q$, which implies that (34) will be zero and therefore the state e'_d can either be removed from the model or be replaced by the equivalent sub-transient state e''_d. For a description of the synchronous machine parameters for different winding configurations and their typical values, the reader is referred to [23].

In (36), the mechanical power P_m, controlled by the turbine governor system, and the field voltage E_{fd}, controlled by the excitation system, are in general not available as real-time measurements outside the the power plant. If accurate models of the control systems are known, the estimation model could be extended with these controllers with the intent to improve the estimates. However, the controllers can change due to, for example, the activation of over-/under-excitation limiters, varying parameters, or malfunctioning equipment. Furthermore, even if the models are known, unknown input estimation might still have to be used because the controllers could have set-points that are unknown or have inputs that are not available as measurements, e.g. the inputs to power system stabilizers. For these reasons, this paper assumes that only the synchronous machine's parameters are known.

A. ESTIMATION MODEL USED BY EKF-UI

A complication of using the state vector (35) directly in EKF-UI is that the machine angle δ is taken with respect to a fictitious slack bus. This limitation was avoided in the estimation model of [5], which proposed to extend the state vector (35) with an extra state $x_5 = \delta_i$, the internal machine angle. The internal machine angle δ_i is computed with respect to the voltage phasor V_t at the machine's terminal bus. As a state equation for δ_i, the equation $\dot{\delta}_i = \dot{\delta}_c$ is used by [5], where δ_c is calculated [23] as

$$\delta_c = \tan^{-1}\left(\frac{x_q I_t\cos(\phi) - R_a I_t\sin(\phi)}{V_t + R_a I_t\cos(\phi) + x_q I_t\sin(\phi))}\right), \quad (39)$$

where $\phi = \cos^{-1}\left(\frac{P_t}{V_t I_t}\right)$ is the phase angle between voltage and current. The quantities that are needed in order to calculate (39) are the PMU-measurements $\bar{V}_t$ and $\bar{I}_t$ and the machine parameters x_q, R_a, which are assumed to be known. To obtain observability of the second state x_2, i.e. the rotor speed deviation $\Delta\omega$, an approximate measurement of the rotor speed is needed. In [5], the estimated speed f_r of the q-axis internal voltage phasor $\bar{E}_q = \bar{V}_t + jx_q\bar{I}_t$ is used. This quantity can be calculated from measured phasor quantities, obtained from PMU devices at the terminal bus, and knowledge of the q-axis reactance of the machine. Following the description in [5], the EKF-UI will for the fourth-order synchronous machine model use the state vector $x_k = [\delta\ \Delta\omega\ e'_q\ e'_d\ \delta_i]^T$, input vector $u_k = [V_t\ \delta_c]^T$ and the output is $y_k = [P_e\ Q_e\ f_r]^T$, where δ_c is calculated by (39) and f_r is the frequency of the q-axis voltage phasor $\bar{E}_q$ given by $\bar{E}_q = \bar{V}_t + jx_q\bar{I}_t$, where $\bar{V}_t$ and $\bar{I}_t$ can be obtained as PMU measurements at the machine's bus [5].

B. PROPOSED ESTIMATION MODEL FOR NERTSS

The estimation model described in Section III-A has two potential issues. First, the size of the state vector is increased by one, such that the algorithm must calculate more estimates from a fixed amount of measurements. Second, the measurement errors in u_k, which is also augmented by an additional measurement, may potentially degrade estimation performance. The second issue arises from the use of the calculated internal machine angle δ_c of (39), which can be sensitive to measurement errors in V_t, I_t and ϕ.

To avoid these two potential issues, the estimation model of [5] is reformulated to avoid using δ_c while still being able to estimate δ_i. For this purpose, the first state of (35), i.e. δ, is replaced by the internal machine angle δ_i. The internal machine angle δ_i is the angle in radians between the d-axis of the rotor and the local bus voltage phasor $\bar{V}_t$, and evolves over time by integrating the difference between the electrical speed f_e and mechanical speed ω. The state equation for x_1 in (31) is therefore substituted with

$$\dot{x}_1 = \omega_0\,(x_2) - 2\pi(f_e - f_n) \quad (40)$$

where $f_e - f_n$ is the deviation in Hertz of the electrical frequency from the nominal value and $\omega_0 = 2\pi f_n$. Thus, the proposed estimation model for the NERTSS uses $[\delta_i\ \Delta\omega\ e'_q\ e'_d]^T$ as the state vector, $u_k = [V_t\ f_e]^T$ as the input vector, and $y_k = [P_e\ Q_e\ f_r]^T$ as the output vector.

IV. NOISE MODELING FOR THE NUMERICAL EXPERIMENTS

An important part of the experiment design is the choice of noise sources to account for imperfect modeling of the synchronous machine and the imperfect measurements. In the experiments, all noise sources are modeled as an additive white Gaussian noise (AWGN) and being zero mean and jointly uncorrelated. The following noise injections are made:

- **Process noise** attributed to modeling and discretization errors by approximating the state function (1) by $f_k(x_k, d_k, u_k)$. The process noise is taken into account by injecting noise into the each state of the estimation model. The noise sources are assumed to be uncorrelated AWGN that are each distributed by $\mathcal{N}(0, 10^{-10})$ before time-discretization. The discrete-time covariance is approximated as the continuous-time covariance multiplied by the the square of the simulation time-step.

The variance of the considered process noise is therefore slightly higher than the variance used in [9].

- **Measurement noise** attributed to modeling errors by approximating the measurement function (2) by $g_k(x_k, u_k)$. The measurement noise is added to each of the measurement equations of the estimation models. The noise sources are assumed to be uncorrelated, AWGN and distributed by $\mathcal{N}(0, 10^{-10})$. The variance of the measurement noise is two orders of magnitude larger than the variance used in [9].
- **Instrument noise**, due to imperfect PMU-measurements, affecting u_k which enters nonlinearly into both state and measurement equations (1),(2). To account for instrument noise, the IEEE C37.118.1-2011 standard for synchrophasors [24] allows up to 1% total vector error (TVE) for voltage and current measurements, respectively, for both P class and M class PMUs during steady-state. These errors may be compounded by the measurement transformer errors which are, depending on the accuracy class of the instrument, restricted to not deviate more than 0.3% and 1.2% [25]. Using these deterministic accuracy bounds as a guideline, the errors in the measured per-unit phasor quantities $\bar{V}$ and $\bar{I}$ are modeled by uncorrelated AWGN sources with their respective magnitudes distributed as $\mathcal{N}(0, 10^{-6})$ (pu) and phase distributed by the uniform distribution on $[0, 2\pi]$ (rad). The quantiles of the considered current and voltage noise distributions correspond to a case when the respective measurements have an expected TVE that is less than 1% for approximately 99.99% of the samples when the current and voltage magnitude are 1 pu, respectively. For frequency measurements f_e, note that the frequency error is not allowed to exceed 0.005 or 0.01 Hz depending on the accuracy class [24]. The paper takes the higher bound into account and model the frequency measurement error as an AWGN source with the distribution $\mathcal{N}(0, 10^{-6})$ Hz.

V. NUMERICAL EXPERIMENTS

The performance of the EKF-UI and NERTSS estimation methods are numerically investigated by performing Monte Carlo simulations for several different experiments.

First, the algorithms' estimation is investigated in several case studies using the fourth-order machine models of the 60-Hz WSCC 9-bus test system as implemented in PSAT [26]. Second, experiments are carried out investigate the algorithms' ability to estimate the states and inputs of higher-order machine models having salient poles. These latter case studies include the impact of electromagnetic transients by using the simplified Hydro-Quebec system as implemented in the Simulink Simscape Power Systems toolbox [5].

The estimation models used by the EKF-UI and the NERTSS are, respectively, described in Section III and kept as order four regardless of the model order of the simulated machine. The input and output vectors used by the estimation methods are obtained using only noisy PMU measurements $\bar{V}_t, \bar{I}_t$ and f_e. The expressions for the time-varying Jacobian matrices (8), (9) and (13), which are needed in both EKF-UI and NERTSS, are assumed to be known analytically from differentiating the estimation models. However, the numerical values of the Jacobian matrices are calculated from the machine parameters, the noisy phasor measurements and the state estimates. Thus, the numerical values of the Jacobian matrices will differ from the true values. To ensure fairness in the comparisons, the same Q and R matrices were used for both methods by using the diagonal covariance matrices $R = Q = 10^{-5}I$ where I are identity matrices of appropriate sizes. The initial estimates of state and unknown input, needed to start the recursion, are the true underlying values perturbed by three standard deviations of the state covariance matrix.

As in [5], a Kay-filter [27] applied over a window of 1.5 cycles is used to calculate the rotor speed f_r. The assumed reporting rate of the PMU devices including the rotor angle calculation algorithm is two samples per cycle, i.e. 8 $^1/_3$ ms. Compared to [5], the assumed reporting rate in this paper is lower by a factor of 12. The lower reporting rate could make the estimation problem harder, because the errors caused by linearizing the state equations grow when the sampling rate is decreased. Note that, due to the high reporting rate and the approximate unbiasedness of the estimates, there is an opportunity to use averaging to reduce the variance before presenting the unknown input estimates. However, this paper presents only unprocessed estimates in all figures and tables unless it is explicitly stated. For the NERTSS algorithm, it should be noted that the paper only presents the filtered state estimates and not the smoothed state estimates in order to avoid a delay by one time-step.

The performance metric is the mean square error (MSE) of the estimate $\hat{z}[n]$ with respect to the simulated variable $z[n]$, defined as

$$\mathrm{MSE}(\hat{z}) = \frac{1}{N}\sum_{n=1}^{N}\left(z[n] - \hat{z}[n]\right)^2, \tag{41}$$

where N is the number of samples. The reported MSE values are calculated per estimated quantity as the average of 100 Monte Carlo simulations with different noise realizations. To test whether it is possible to reject the null hypothesis that the average MSE of the two methods are equal, Welch's two-tailed t-test with a probability value of $p = 0.01$ is used. This test assumes that the MSEs for both of the methods are, respectively, normal distributed and allows the two distributions to have unequal variances.

A. PERFORMANCE UNDER AMBIENT CONDITIONS WITH STOCHASTICALLY VARYING LOADS

Case study V-A seeks to track the states and inputs of a regulating generator as it is following the changes in consumption during normal operation. The changes in active and reactive power consumption at the load buses are modeled

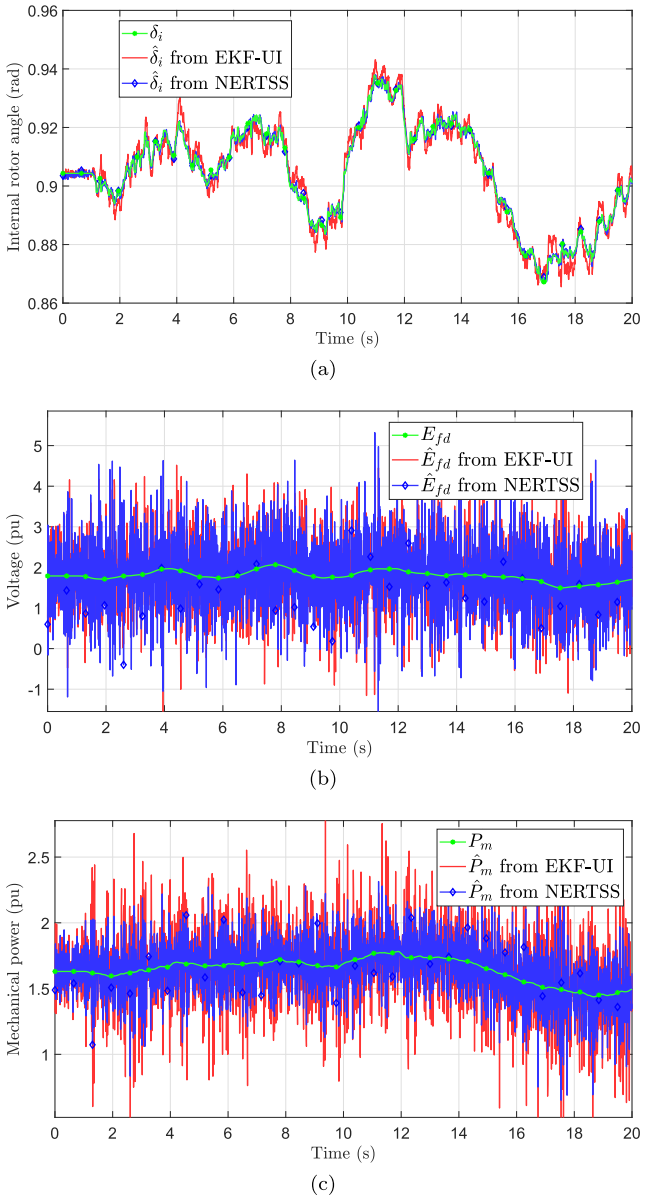

FIGURE 1. Case study V-A: Estimates produced by the EKF-UI (red) and the NERTSS (black) and the true machine states and inputs (green). (a) Internal machine angle δ_i. (b) Field voltage E_{fd}. (c) Mechanical power P_m.

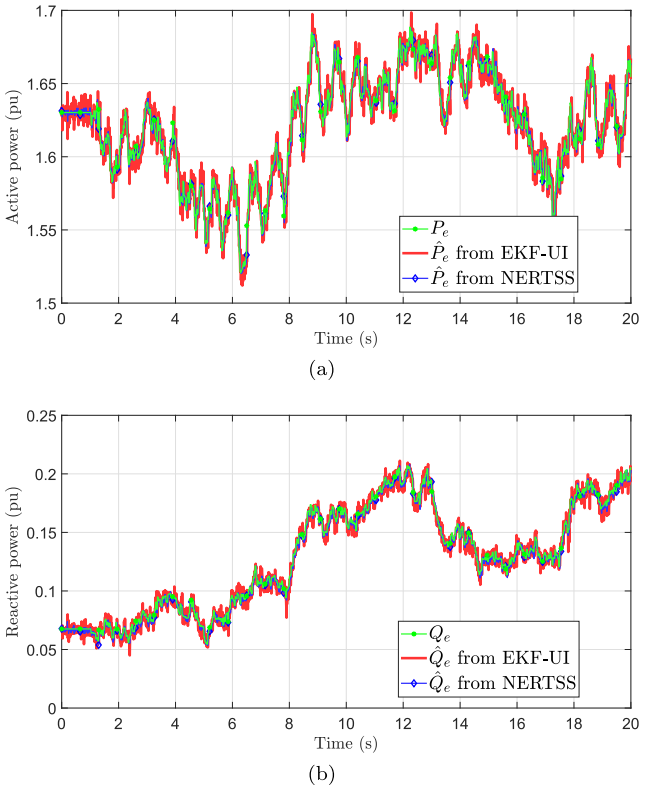

FIGURE 2. Case study V-A: Estimated outputs calculated from the EKF-UI (red) and the NERTSS (black) estimates and the true machine outputs (green). (a) Active power P_e. (b) Reactive power Q_e.

TABLE 1. Case study V-A: Average estimation performance from 100 Monte Carlo simulations. The best average MSE values are in bold if the result is significant with $p = 0.01$ using Welch's two-tailed t-test.

Average MSE	EKF-UI	NERTSS
$\hat{\delta}$ [rad]	1.338×10^{-5}	$\mathbf{1.139 \times 10^{-5}}$
$\widehat{\Delta\omega}$ [pu]	4.248×10^{-8}	$\mathbf{3.733 \times 10^{-8}}$
$\hat{e}'_q$ [pu]	5.064×10^{-6}	$\mathbf{7.875 \times 10^{-7}}$
$\hat{e}'_d$ [pu]	7.256×10^{-6}	$\mathbf{5.489 \times 10^{-8}}$
$\hat{E}_{fd}$ [pu]	8.163×10^{-1}	$\mathbf{7.608 \times 10^{-1}}$
$\hat{P}_m$ [pu]	1.266×10^{-1}	$\mathbf{8.808 \times 10^{-2}}$

with zero-drift Wiener processes having a variance of 0.01 pu after time-discretization. The instantaneous net consumption of power in the loads is therefore deviating from what was anticipated in the planning stage and can be thought of as the aggregate time-varying demand of the loads or as the varying production of unschedulable distributed generation. Fig. 1 shows, for a single simulation, the estimated states and unknown inputs that were calculated by the two methods and compares them with the true values. From Fig. 1, it is clear that the NERTSS have a smaller MSE than the EKF-UI for the internal rotor angle estimation as well as the mechanical power and field voltage unknown input estimates. It can also be seen that the unknown input estimates vary around the true underlying values, showing that the estimates are approximately unbiased.

Fig. 2 shows, for a single simulation, the active and reactive power output of the machine when reconstructed using the estimated states compared to the true values. It can be seen that the active power is reconstructed by the NERTSS with less error than the EKF-UI, while the accuracy is similar for both methods when the reactive power is to be reconstructed.

To numerically assess the performance of the algorithms during ambient conditions, 100 Monte Carlo simulations are carried out and the average MSE is calculated for all simulations for which the estimates are bounded. The results are presented in Table 1 and show that both methods perform

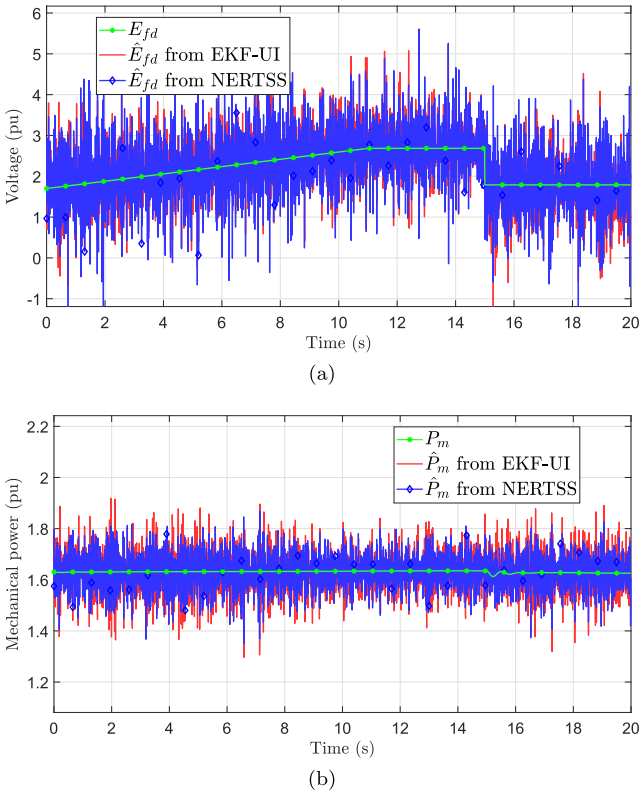

FIGURE 3. Case V-B.1: Estimates produced by the EKF-UI (red) and the NERTSS (black) compared to the true machine inputs (green) for (a) Field voltage E_{fd}. (b) Mechanical power P_m.

well for the state estimation, keeping the estimation errors small for all states. For the unknown inputs to the machine, the NERTSS is performing better than the EKF-UI when it comes to estimating both the mechanical power input as well as the field voltage input.

B. PERFORMANCE TRACKING RAMPS AND STEPS IN THE UNKNOWN INPUTS

Case study V-B carries out two experiments which investigates the algorithms' ability to track time-varying unknown inputs. The reference signal consists of a ramp at $t = 0$ s that increases the studied unknown input by 50% over 10 s, after which it is held constant for 5 s before applying a negative step that resets the input to its initial value. The Monte Carlo simulation procedure, used to calculate the average MSEs and to carry out the significance tests, is the same as the one in case study V-A.

1) RAMP AND STEP IN THE FIELD EXCITATION VOLTAGE

Case V-B.1 applies the reference signal to the field excitation voltage E_{fd} of the synchronous machine. The plots in Fig. 3 show that both algorithms track the input signals, i.e. the field voltage and mechanical power, reasonably well for this disturbance but that the NERTSS will do so with lower variance than the EKF-UI.

Table 2 presents the average MSEs of the estimates obtained from the respective algorithm using

TABLE 2. Case study V-B.1: Average estimation performance from 100 Monte Carlo simulations. The best average MSE values are in bold if the result is significant with $p = 0.01$ using Welch's two-tailed t-test.

Average MSE	EKF-UI	NERTSS
$\hat{\delta}$ [rad]	3.188×10^{-5}	$\mathbf{2.003 \times 10^{-7}}$
$\widehat{\Delta\omega}$ [pu]	2.745×10^{-9}	2.085×10^{-9}
$\hat{e}'_q$ [pu]	1.153×10^{-5}	$\mathbf{6.286 \times 10^{-7}}$
$\hat{e}'_d$ [pu]	5.553×10^{-5}	$\mathbf{1.459 \times 10^{-7}}$
$\hat{E}_{fd}$ [pu]	4.160×10^{-2}	$\mathbf{3.510 \times 10^{-2}}$
$\hat{P}_m$ [pu]	4.934×10^{-3}	$\mathbf{2.805 \times 10^{-3}}$

TABLE 3. Case V-B.2: Average estimation performance from 100 Monte Carlo simulations. The best average MSE values are in bold if the result is significant with $p = 0.01$ using Welch's two-tailed t-test.

Average MSE	EKF-UI	NERTSS
$\hat{\delta}$ [rad]	1.010×10^{-4}	$\mathbf{2.443 \times 10^{-6}}$
$\widehat{\Delta\omega}$ [pu]	7.579×10^{-8}	$\mathbf{7.538 \times 10^{-8}}$
$\hat{e}'_q$ [pu]	5.022×10^{-5}	$\mathbf{9.099 \times 10^{-7}}$
$\hat{e}'_d$ [pu]	6.867×10^{-5}	$\mathbf{5.866 \times 10^{-8}}$
$\hat{E}_{fd}$ [pu]	2.209×10^{-1}	$\mathbf{2.104 \times 10^{-1}}$
$\hat{P}_m$ [pu]	1.448×10^{-3}	$\mathbf{7.050 \times 10^{-4}}$

100 Monte Carlo simulations. The table shows that the NERTSS was on average better than the EKF-UI when estimating the unknown inputs, in particular the mechanical power input to the generator. Furthermore, the NERTSS give better estimates of the states compared to the EKF-UI, except for the rotor speed where no significant difference was observed.

2) RAMP AND STEP IN THE MECHANICAL POWER

Case V-B.2 uses the same reference signal as the one used in case V-B.1, but the reference signal is in this case applied to the mechanical power input to the synchronous machine.

Fig. 4 show estimation results of selected states and unknown inputs compared to the their true values. Note that the NERTSS method manages to track the inputs with a relatively small estimation error and a low variance, while the EKF-UI method has both higher estimation errors and larger variance. The biggest contributor to the estimation errors in case V-B.2 can be seen to be the oscillations in the unknown input estimates that are induced by the step change, this problem is common to both the NERTSS and the EKF-UI and could be addressed by enhanced linearization techniques. As can be seen in Table 3, the NERTSS algorithm performs better than the EKF-UI for all estimated quantities.

C. PERFORMANCE DURING FAULT CONDITIONS

Case study V-C tests the algorithms' ability to track the transient behavior of the states and unknown inputs of synchronous machines during fault conditions. The considered

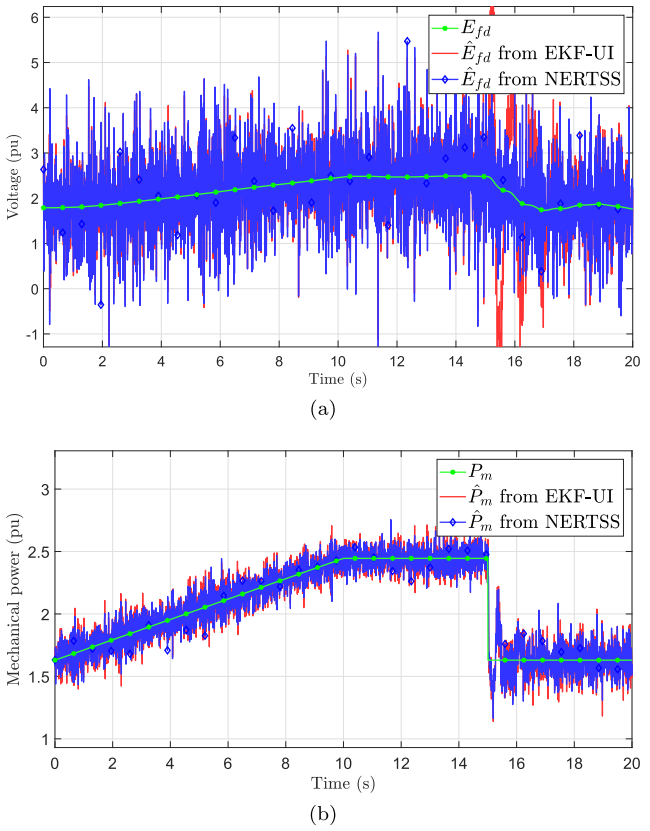

FIGURE 4. Case V-B.2: Unknown input estimates produced by the EKF-UI (red) and the NERTSS (black) compared to the true machine inputs (green). (a) Field voltage E_{fd}, (b) Mechanical power P_m.

fault is a balanced three-phase-to-ground fault applied to the bus which connects the monitored machine with the rest of the grid. The fault is applied at $t = 1$ s and is cleared after 200 ms. The fault impedance is set to be $\bar{Z}_f = j0.1$ pu and the simulations are carried out until $t = 5$ s, at which time the oscillations in the states have almost completely disappeared.

Fig. 5 shows that during the fault both algorithms are unsuccessful at tracking the unknown inputs during the fault, while the NERTSS is able to estimate the rotor angle correctly. The failure of the EKF-UI to correctly estimate the internal rotor angle during the fault is caused by the use of (39), which is the steady-state value that may differ from the true value during transients. Both methods give unknown input estimates during the faults that are unsuitable to be used directly for monitoring purposes. After the fault is cleared, the unknown input estimates of the NERTSS is faster to converge to the true underlying system's response than the EKF-UI, the latter of which exposes large oscillations when estimating the mechanical power input to the synchronous machine. The lack of estimation accuracy during faults is not surprising and similar results for the EKF-UI were reported in [5].

In Table 4, the average MSE obtained from 100 Monte Carlo simulations are given. Table 4 shows that the NERTSS performs better than the EKF-UI for all of the estimates. However, the MSE of the unknown input estimates are very

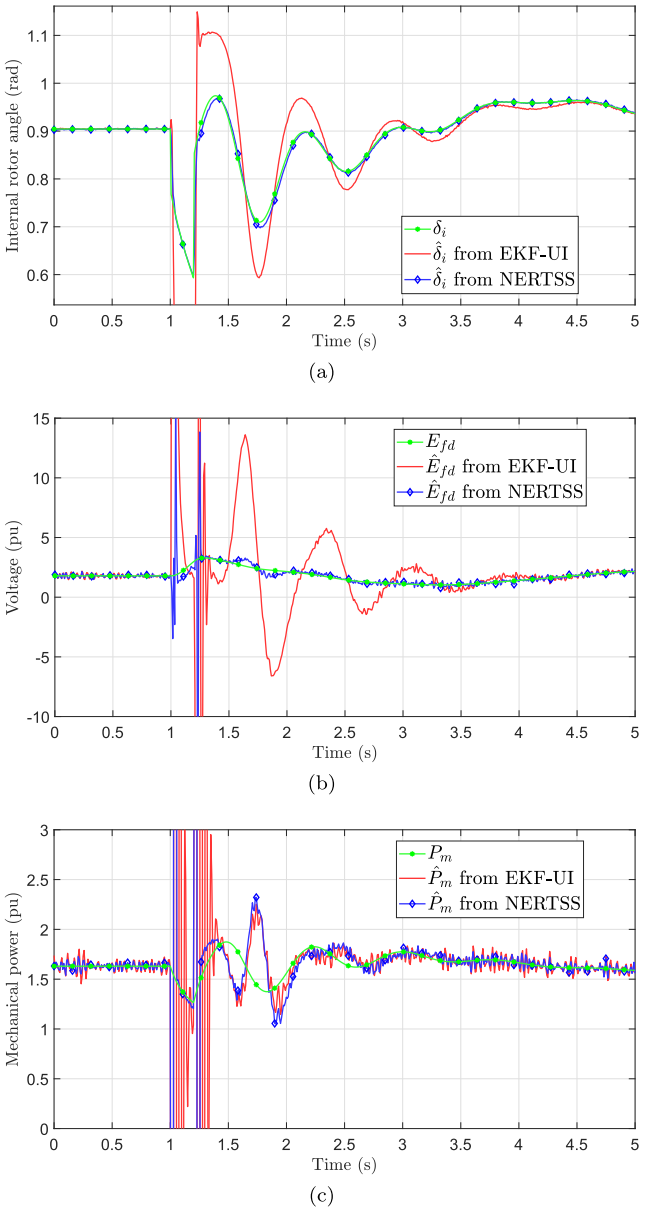

FIGURE 5. Case study V-C: Estimates produced by the EKF-UI (red) and the NERTSS (blue) compared to the true machine states and inputs (green). (a) Internal rotor angle δ_i, (b) Field voltage E_{fd}, (c) Mechanical power P_m.

large for both algorithms and is mainly due to the inaccurate results during the fault.

D. INFLUENCE OF THE ESTIMATION MODEL ON THE NERTSS' ESTIMATION PERFORMANCE

Case study V-D performs a comparative study the two estimation models presented in Section III by evaluating the estimation accuracy when the estimation model is used by the NERTSS. The experimental set-up of case study V-A was used to calculate the average MSE obtained with the respective estimation model. The results of the Monte Carlo simulations are reported in Table. 5. As can be seen from the average MSE, the new estimation model proposed in Section III-B is the preferred option for use with the NERTSS.

TABLE 4. Case study V-C: Average estimation performance from 100 Monte Carlo simulations. The best average MSE values are in bold if the result is significant with $p = 0.01$ using Welch's two-tailed t-test.

Average MSE	EKF-UI	NERTSS
$\hat{\delta}$ [rad]	5.910×10^{-3}	$\mathbf{1.702 \times 10^{-4}}$
$\widehat{\Delta\omega}$ [pu]	2.343×10^{-5}	$\mathbf{1.898 \times 10^{-5}}$
$\hat{e}'_q$ [pu]	1.447×10^{-3}	$\mathbf{5.902 \times 10^{-6}}$
$\hat{e}'_d$ [pu]	3.886×10^{-3}	$\mathbf{3.317 \times 10^{-5}}$
$\hat{E}_{fd}$ [pu]	58.99	**1.894**
$\hat{P}_m$ [pu]	39.18	**21.31**

TABLE 5. Case study V-D: Average estimation performance depending on the estimation model used by NERTSS from 100 Monte Carlo simulations. The best average MSE values are in bold if the result is significant with $p = 0.01$ using Welch's two-tailed t-test.

Average MSE	Model III-A	Model III-B
$\hat{\delta}$ [rad]	8.665×10^{-6}	$\mathbf{7.880 \times 10^{-7}}$
$\widehat{\Delta\omega}$ [pu]	2.452×10^{-8}	$\mathbf{1.832 \times 10^{-8}}$
$\hat{e}'_q$ [pu]	3.675×10^{-6}	$\mathbf{7.918 \times 10^{-7}}$
$\hat{e}'_d$ [pu]	4.747×10^{-6}	$\mathbf{4.614 \times 10^{-8}}$
$\hat{E}_{fd}$ [pu]	8.371×10^{-1}	$\mathbf{7.706 \times 10^{-1}}$
$\hat{P}_m$ [pu]	5.743×10^{-2}	$\mathbf{4.311 \times 10^{-2}}$

When using the same estimation model, the NERTSS is performing better than the EKF-UI for all estimates except for the field voltage, which showed no significant difference in accuracy between the two algorithms. These results show that the improvement in estimation accuracy of the NERTSS compared to the EKF-UI is partially due to the proposed estimation model and partially due to the NERTSS algorithm.

E. ESTIMATION FOR HIGHER-ORDER MACHINE MODELS IN THE HYDRO-QUEBEC SIMPLIFIED SYSTEM

To conclude the case studies, the paper investigates the ability of the NERTSS and the EKF-UI algorithms to use a simplified estimation model of order 4 when estimating unknown inputs and states of a salient-pole synchronous machine with a model order of 8.

Similar experiments were carried out for the EKF-UI in [5], using the same Simulink model of the simplified Hydro-Quebec 29-bus system. Therefore, the experiment set-up is chosen to match that of [5] as closely possible. However, this case study differs from those of [5] by considering noise sources that are affecting the output of the PMU measurements. Furthermore, the PMUs used in this paper are based on phase-locked loops, which differs from the PMU implementation in [5].

Fig. 6 shows the simplified Hydro-Quebec system as it is implemented in the Simulink environment, including the block containing the PMUs and the rotor speed estimator, and the blocks containing the estimation algorithms. The synchronous machine **MTL**, whose unknown inputs and states

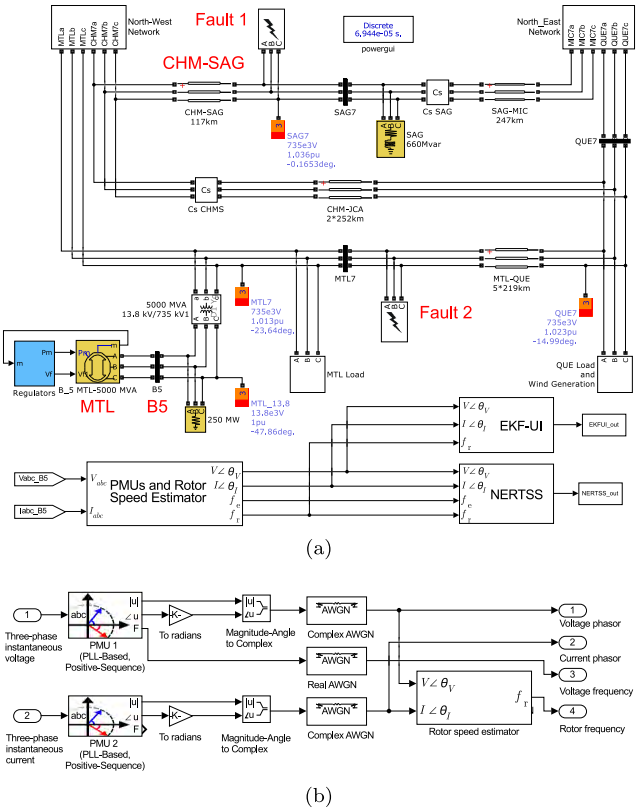

FIGURE 6. Case study V-E: (a) The simplified 29-bus Hydro-Quebec system and the blocks containing the estimation algorithm, and (b) implementation of the PMU, instrument noise and the rotor speed estimator.

are to be estimated, is shown in the left part of Fig. 6, connected to bus **B5**, where the PMUs measuring $\bar{V}_t$ and $\bar{I}_t$ are located.

The system is simulated with a time-step of $(240 \times 60)^{-1}$s $\approx 69\mu$s, which is considerably faster than the assumed synchrophasor sampling rate of 24 samples per cycle. The reporting rates of the PMUs and the rotor speed estimator are all assumed to be 2 samples per cycle. The two considered cases investigate the accuracy of the algorithms when they are using simplified estimation models and noisy PMU data as the system is subjected to faults.

1) A REMOTE THREE-PHASE-TO-GROUND SHORT-CIRCUIT FAULT

In this case, a balanced three-phase-to-ground short-circuit fault is applied to the line **CHM-SAG** in the upper left corner of Fig. 6 as **Fault 1**. This fault is electrically located far away from the monitored machine **MTL**. Therefore, it should be expected that the influence of the sub-transient dynamics should be limited, since there is a comparatively large amount of impedance between the machine and the fault [23].

Fig. 7 shows the selected estimated states and the estimated unknown inputs for a noise realization. It can be seen from the plot that both algorithms accurately estimate the internal rotor angle δ_i even during the fault. In contrast, the unknown input

TABLE 6. Case study V-E.1: Average estimation performance from 100 Monte Carlo simulations. The best average MSE values are in bold if the result is significant with $p = 0.01$ using Welch's two-tailed t-test.

Average MSE	EKF-UI	NERTSS
$\hat{\delta}$ [rad]	3.773×10^{-4}	$\mathbf{4.679 \times 10^{-5}}$
$\widehat{\Delta\omega}$ [pu]	1.009×10^{-6}	$\mathbf{7.323 \times 10^{-7}}$
$\hat{E}_{fd}$ [pu]	3.814	**3.474**
$\hat{P}_m$ [pu]	1.286×10^{-2}	$\mathbf{1.198 \times 10^{-2}}$

estimates are seen to be unreliable during the fault. After the fault has been cleared, the field voltage estimate converges very quickly to the true underlying value. When the algorithms estimate the mechanical power input in the transient time-period after the fault, both the NERTSS and the EKF-UI exhibit oscillations that are damped out after a few seconds. These are introduced as the algorithms try to compensate for the difference between predicted and observed measurements.

In Table 6, the calculated MSEs obtained from the Monte Carlo-simulations are showing that the NERTSS has slightly better accuracy than the EKF-UI for the state and unknown input estimates in the case of a remote fault. Note that the transient d- and q-axis voltages are not investigated in the case studies for the simplified Hydro-Quebec system, as their reference values are not directly available as states of the eighth-order machine model.

2) A NEARBY THREE-PHASE-TO-GROUND SHORT-CIRCUIT FAULT

In this case, the balanced three-phase-to-ground short-circuit fault is located at the point of interconnection between the monitored machine and its transformer on one side and the rest of the grid on the other side, shown as **Fault 2** in Fig. 6. The impedance between the fault and the machine is comparatively small and the machine's sub-transient dynamics should therefore have a large impact on the states and unknown inputs of the machine.

As can be seen in Fig. 8, the errors in the unknown input estimates are large during the fault and immediately after the fault has been cleared. Note that the EKF-UI algorithm tracks the internal rotor angle better than the NERTSS during the fault and slightly worse after the fault, which can be explained by the inaccurate frequency calculation by the PMU during the fault. After the fault is cleared, the field voltage estimates converge to the reference signal and track the oscillations well. In contrast, the mechanical power estimates exhibit damped oscillations and high frequency noise during the first few seconds after clearing the fault. This is partially due to the part of the dynamics of the machine that is not taken into account in the estimation model, which then noticeably affects the unknown input estimates.

In Table 7, the average estimation errors are presented and which show that the NERTSS performs slightly better than the EKF-UI for most of the estimates. As was

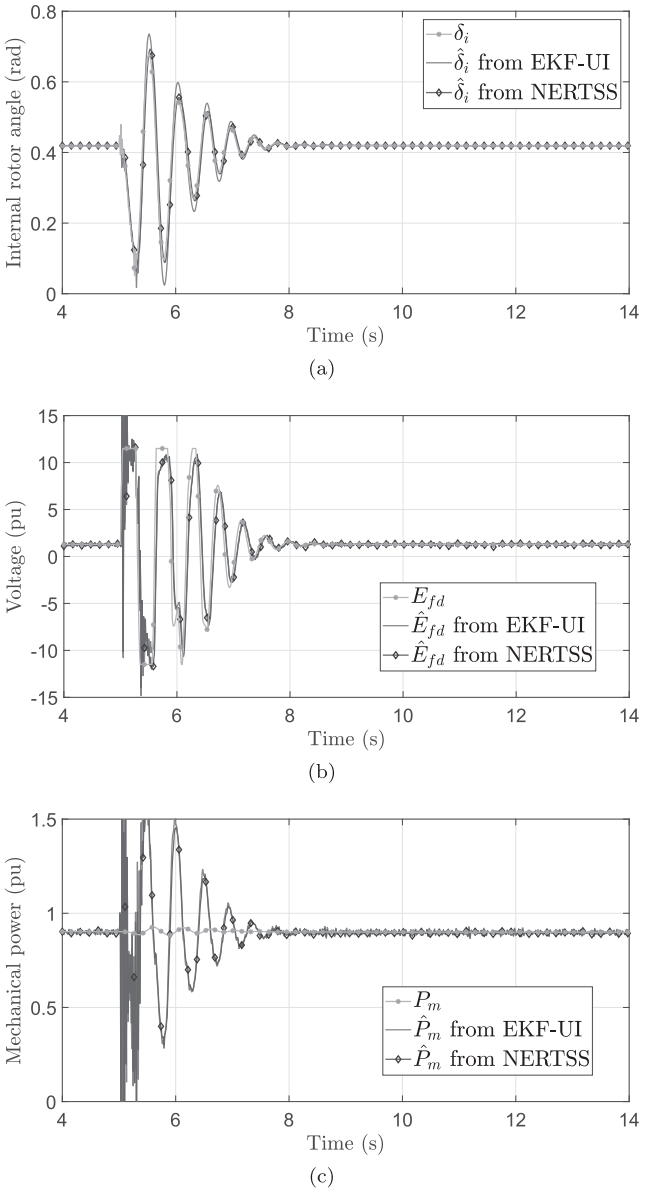

FIGURE 7. Case study V-E: Estimates produced by the EKF-UI (red) and the NERTSS (blue) compared to the true machine states and inputs (green). (a) Internal rotor angle δ_i, (b) Field voltage E_{fd}, (c) Mechanical power P_m.

observed from Fig. 8, the internal rotor angle calculation of the EKF-UI, gives the EKF-UI and advantage over the NERTSS when the frequency measurements from PMUs are unreliable due to the fault. Note that the large estimation errors during the under-fault conditions are the main contributors to the high MSEs. However, for the unknown inputs, the relative accuracy of the two algorithms are similar even if only the post-fault time period is considered.

VI. COMPUTATIONAL PERFORMANCE AND APPLICATIONS

A. COMPUTATIONAL PERFORMANCE

For real-time applications, the computational cost of the algorithms is important and the computation time should

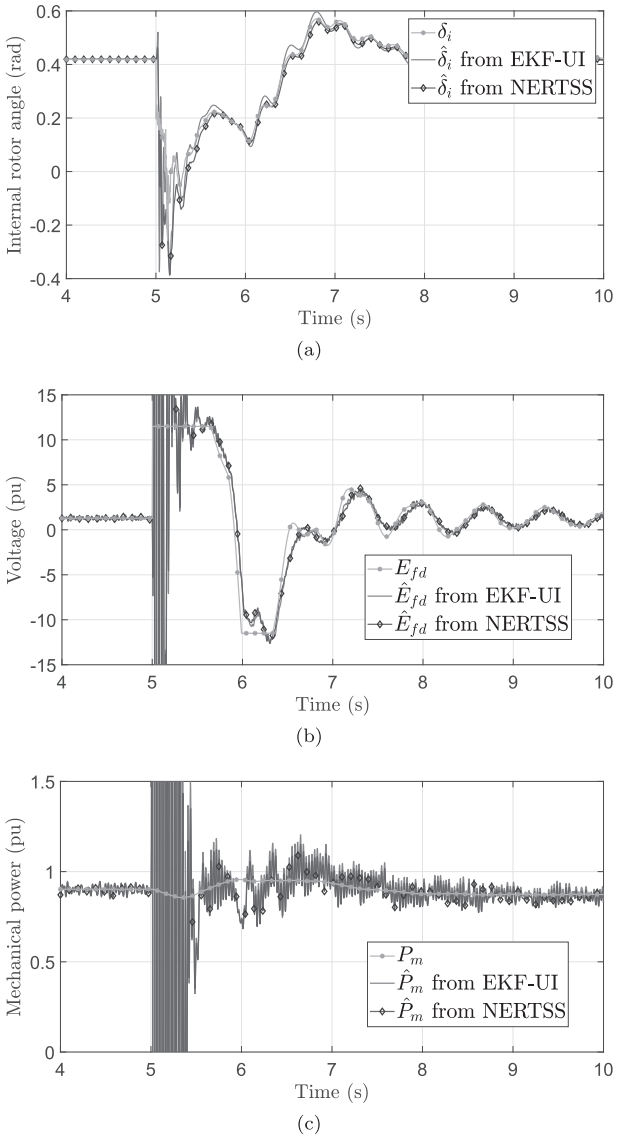

FIGURE 8. Case study V-E.2: Estimates produced by the EKF-UI (red) and the NERTSS (blue) compared to the true machine states and inputs (green). (a) Internal rotor angle δ_i, (b) Field voltage E_{fd}, (c) Mechanical power P_m.

TABLE 7. Case study V-E.2: Average estimation performance from 100 Monte Carlo simulations and calculated after the fault has been cleared. The best average MSE values are in bold if the result is significant with $p = 0.01$ using Welch's two-tailed t-test.

Average MSE	EKF-UI	NERTSS
$\hat{\delta}$ [rad]	$\mathbf{2.088 \times 10^{-3}}$	2.494×10^{-3}
$\widehat{\Delta\omega}$ [pu]	2.638×10^{-5}	$\mathbf{2.295 \times 10^{-5}}$
$\hat{E}_{fd}$ [pu]	3.789×10^{2}	$\mathbf{3.746 \times 10^{2}}$
$\hat{P}_m$ [pu]	4.119×10^{1}	$\mathbf{2.749 \times 10^{1}}$

be well below the reporting rate of the synchrophasor data. The operations with most computational cost in EKF-UI and NERTSS are the matrix inversions that need to be performed at every time step. The covariance matrices that are inverted are of comparable size for the two methods. It should therefore be expected that the NERTSS would have a similar computational cost as that of the EKF-UI, as the NERTSS only requires one extra matrix inversion per time step.

To investigate the practical computational cost, the average computational time for a single step of the NERTSS and the EKF-UI, respectively, was calculated using 10,000 estimation steps for each algorithm. The implementation of the EKF-UI, developed in MATLAB for this work, was found to give an average computational time of 2.6 ms per step. In comparison, the implementation of the NERTSS in MATLAB took on average 7.2 ms per step. Thus, the computational cost is lower for the EKF-UI. However, both algorithms can easily complete a single step within a reporting rate of 2 samples per cycle, consistent with the reporting rate of a modern PMU.

Software profiling of the NERTSS and the EKF-UI algorithms revealed that both algorithms spent most of the time evaluating the partial derivative matrices of the state and measurement functions, note that these matrices are needed for both the EKF-UI and the NERTSS. This partially explains the observed difference in computation time between the two methods because the NERTSS is evaluating the partial derivative matrices twice per time step instead of once, which the case for the EKF-UI. The partial derivative evaluation could likely be made considerably faster by creating a more light-weight implementation than the one that was used in the experiments, which was written in the interpreted MATLAB language and allows the user to modify parameters during simulations. The numerical experiments of [9] showed that the EKF-UI can be executed on a standard personal computer at a rate that was two magnitudes faster than the considered PMU reporting rate which, considering the similar computational cost, also supports the conclusion that the NERTSS can be implemented to run in real-time.

B. APPLICATION TO FREQUENCY CONTROL PERFORMANCE MONITORING

Monitoring the primary reserves of the power system is important task in order to ensure that excessive frequency deviations does not occur. In steady-state, the regulating machines have a frequency response that is inversely proportional the droop parameter R, which can be tracked with relatively slow SCADA systems. To obtain a faster reporting rate with lower latency, this paper proposes to use of PMU data and the NERTSS algorithm to estimate the mechanical power input P_m and the rotor speed ω of the generator. These quantities can then be used to track the performance of the primary frequency control loop. The higher update rate compared to SCADA systems means that warnings to system operators could be presented in a more timely manner if the primary frequency reserves would deviate from the scheduled amount.

An example under ambient conditions is shown in Fig. 9, where the estimated points in the P_m-ω space are shown to be close to the theoretical steady-state droop of the turbine governor. It can be observed in Fig. 9 that the turbine regula-

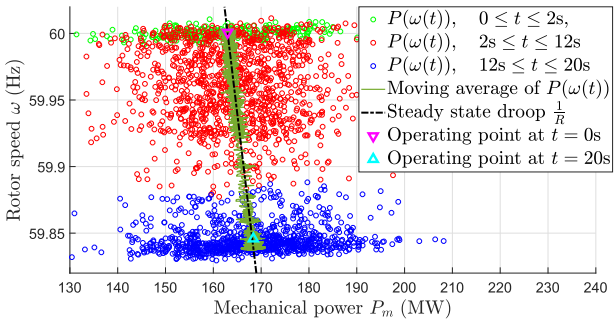

FIGURE 9. Application example VI-B: Frequency control performance monitoring, the estimated operating points from the NERTSS compared to the steady-state droop.

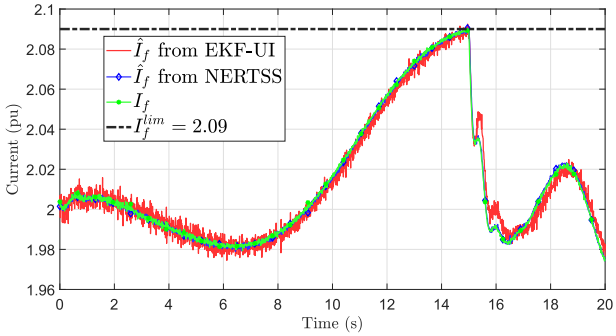

FIGURE 10. Application example VI-C: Field current tracking, the estimates from the EKF-UI (red) and the NERTSS (black) compared to the true value (green).

tor increases the mechanical power that the turbine delivers to the generator when the rotor speed is decreased, which in turn is caused by the increased loading of the system. As these values are being estimated in real-time, the behavior of the droop presents an opportunity for system operators the observe the controllers' performance. In Fig. 9, it can be seen that the observed droop, calculated as a moving average over a 10 sample window, is able tracking the theoretical steady-state droop closely. If the observed droop is differing from the scheduled steady-state droop, the deviation from the ideal droop characteristic can be used to identify if the frequency regulation of power plant units are inactive or malfunctioning.

C. APPLICATION TO FIELD CURRENT MONITORING

As described in the introduction, another interesting use case is keeping track of the field current I_f in the field winding of the synchronous machine, which was suggested in [4]. Typically an over-excitation limiter is used to prevent the field winding from over-heating from excessive field currents, and anticipating the activation of such a limit can be of interest for the stability assessment and/or to initiate a redispatch to alleviate the over-excitation.

In Fig. 10, the real field current and its estimates are shown for a scenario where the over-excitation limiter becomes active at $t = 15$ s after a continuous load increase has driven the field current up to the maximum allowed limit $I_f^{lim} = 2.09$ pu. It can be seen that both algorithms are able to track the field current of the synchronous machine but the NERTSS will do so with slightly better accuracy than the EKF-UI in this scenario.

VII. CONCLUSION

This paper has proposed a new estimation algorithm, the NERTSS, for tracking the states and unknown inputs of synchronous generators in the power system. The NERTSS combines the smoothing algorithm of the ULISS with the non-linear filtering of the NERTSF. Estimation of states and unknown inputs can be a useful tool for operators to assess the control performance of the machine and thereby identify potential stability problems.

The proposed NERTSS was for the considered cases in the simulation studies shown to improve the overall estimation accuracy of the unknown inputs, which is the focus of this paper, compared to the EKF-UI. The improvement in accuracy is due to the fact that the NERTSS, in addition to the filtering step, incorporates the information gained from two subsequent state estimates when estimating the unknown input. The estimation accuracy of the NERTSS makes it a promising estimation method for applications that need state and unknown input estimation of synchronous machines, e.g. for wide-area damping control purposes, proposed in [5] and [28].

Since the NERTSS, the EKF-UI and many other estimation algorithms give both means and error covariances for the estimated states and unknown inputs, more advanced developments of these algorithms should also include the uncertainty of the estimated quantities as an output. Incorporating the uncertainties of state and unknown input estimates into safety margin calculations could be a useful way to propose accurate and cost-effective actions to avoid stability problems and to stay within operational constraints.

The proposed NERTSS algorithm does not incur any additional delay in the estimation of the unknown quantities if used in the proposed on-line setting, but it can be also be used in a delayed mode or in an off-line mode which would lead to even better estimation accuracy. The addition of a backward pass to the forward filtering is computationally inexpensive as no partial derivatives are required.

The effects of saturation in synchronous machines should also be included in more advanced estimation models by, for example, approximating the resulting non-analytical Jacobians by using sample-based techniques. The NERTSS algorithm proposed in this paper is a promising starting point for more refined estimators; off-line or delayed smoothing, alternative linearization techniques, and iterated smoothing are interesting topics for future research.

REFERENCES

[1] I. Dobson and L. Lu, "Voltage collapse precipitated by the immediate change in stability when generator reactive power limits are encountered," *IEEE Trans. Circuits Syst. I, Fundam. Theory Appl.*, vol. 39, no. 9, pp. 762–766, Sep. 1992.

[2] A. Del Angel, P. Geurts, D. Ernst, M. Glavic, and L. Wehenkel, "Estimation of rotor angles of synchronous machines using artificial neural networks and local PMU-based quantities," *Neurocomputing*, vol. 70, nos. 16–18, pp. 2668–2678, 2007.

[3] J. K. Mandal, A. K. Sinha, and L. Roy, "Incorporating nonlinearities of measurement function in power system dynamic state estimation," *IEE Proc.-Gener., Transmiss. Distrib.*, vol. 142, no. 3, pp. 289–296, May 1995.
[4] E. Ghahremani and I. Kamwa, "Dynamic state estimation in power system by applying the extended Kalman filter with unknown inputs to phasor measurements," *IEEE Trans. Power Syst.*, vol. 26, no. 4, pp. 2556–2566, Nov. 2011.
[5] E. Ghahremani and I. Kamwa, "Local and wide-area PMU-based decentralized dynamic state estimation in multi-machine power systems," *IEEE Trans. Power Syst.*, vol. 31, no. 1, pp. 547–562, Jan. 2016.
[6] T. Kailath, A. H. Sayed, and B. Hassibi, *Linear Estimation*, vol. 1. Upper Saddle River, NJ, USA: Prentice-Hall, 2000,
[7] S. J. Julier and J. K. Uhlmann, "Unscented filtering and nonlinear estimation," *Proc. IEEE*, vol. 92, no. 3, pp. 401–422, Mar. 2004.
[8] E. Ghahremani and I. Kamwa, "Online state estimation of a synchronous generator using unscented Kalman filter from phasor measurements units," *IEEE Trans. Energy Convers.*, vol. 26, no. 4, pp. 1099–1108, Dec. 2011.
[9] G. Anagnostou and B. C. Pal, "Derivative-free Kalman filtering based approaches to dynamic state estimation for power systems with unknown inputs," *IEEE Trans. Power Syst.*, vol. 33, no. 1, pp. 116–130, Jan. 2018.
[10] K. Emami, T. Fernando, H. H. C. Iu, H. Trinh, and K. P. Wong, "Particle filter approach to dynamic state estimation of generators in power systems," *IEEE Trans. Power Syst.*, vol. 30, no. 5, pp. 2665–2675, Sep. 2015.
[11] N. Zhou, D. Meng, Z. Huang, and G. Welch, "Dynamic state estimation of a synchronous machine using PMU data: A comparative study," *IEEE Trans. Smart Grid*, vol. 6, no. 1, pp. 450–460, Jan. 2015.
[12] P. K. Kitanidis, "Unbiased minimum-variance linear state estimation," *Automatica*, vol. 23, no. 6, pp. 775–778, 1987.
[13] M. Darouach and M. Zasadzinski, "Unbiased minimum variance estimation for systems with unknown exogenous inputs," *Automatica*, vol. 33, no. 4, pp. 717–719, 1997.
[14] M. Hou and R. J. Patton, "Optimal filtering for systems with unknown inputs," *IEEE Trans. Autom. Control*, vol. 43, no. 3, pp. 445–449, Mar. 1998.
[15] C.-S. Hsieh, "Extension of unbiased minimum-variance input and state estimation for systems with unknown inputs," *Automatica*, vol. 45, no. 9, pp. 2149–2153, 2009.
[16] C.-S. Hsieh, "State estimation for nonlinear systems with unknown inputs," in *Proc. 7th IEEE Conf. Ind. Electron. Appl. (ICIEA)*, Jul. 2012, pp. 1533–1538.
[17] S. Z. Yong, M. Zhu, and E. Frazzoli, "Simultaneous input and state smoothing for linear discrete-time stochastic systems with unknown inputs," in *Proc. 53rd IEEE Conf. Decis. Control*, Dec. 2014, pp. 4204–4209.
[18] J. N. Yang, S. Pan, and H. Huang, "An adaptive extended Kalman filter for structural damage identifications II: Unknown inputs," *Structural Control Health Monitor.*, vol. 14, no. 3, pp. 497–521, 2007.
[19] S. Pan, H. Su, P. Li, and Y. Gu, "State estimation for batch distillation operations with a novel extended Kalman filter approach," in *Proc. 48h IEEE Conf. Decis. Control (CDC) Held Jointly 28th Chin. Control Conf.*, Dec. 2009, pp. 1884–1889.
[20] S. Gillijns and B. De Moor, "Unbiased minimum-variance input and state estimation for linear discrete-time systems with direct feedthrough," *Automatica*, vol. 43, no. 5, pp. 934–937, 2007.
[21] S. Z. Yong, M. Zhu, and E. Frazzoli, "A unified filter for simultaneous input and state estimation of linear discrete-time stochastic systems," *Automatica*, vol. 63, pp. 321–329, Jan. 2016.
[22] S. Z. Yong, M. Zhu, and E. Frazzoli, "Simultaneous input and state estimation with a delay," in *Proc. 54th IEEE Conf. Decis. Control (CDC)*, Dec. 2015, pp. 468–475.
[23] P. Kundur, *Power System Stability And Control*. New York, NY, USA: McGraw-Hill, 1994.
[24] *IEEE Standard for Synchrophasor Measurements for Power Systems*, IEEE Standard C37.118.1-2011 (Revision IEEE Std C37.118-2005), Dec. 2011, pp. 1–61.
[25] *IEEE Standard Requirements for Instrument Transformers*, IEEE Standard C57.13-2008 (Revision IEEE Std C57.13-1993), Jul. 2008, pp. c1–c82.
[26] F. Milano, "An Open Source Power System Analysis Toolbox," *IEEE Trans. Power Syst.*, vol. 20, no. 3, pp. 1199–1206, Aug. 2005.
[27] I. Kamwa, M. Leclerc, and D. McNabb, "Performance of demodulation-based frequency measurement algorithms used in typical PMUs," *IEEE Trans. Power Del.*, vol. 19, no. 2, pp. 505–514, Apr. 2004.
[28] A. K. Singh and B. C. Pal, "Decentralized control of oscillatory dynamics in power systems using an extended LQR," *IEEE Trans. Power Syst.*, vol. 31, no. 3, pp. 1715–1728, May 2016.

JAN LAVENIUS was born in Sweden. He received the M.Sc. degree in electrical engineering from the KTH Royal Institute of Technology, Stockholm, Sweden, in 2012, where he is currently pursuing the Ph.D. degree in electrical engineering with the Department of Electric Power and Energy Systems. The main theme of his current research is the development and implementation of estimation methods and machine learning algorithms for power systems applications to facilitate real-time voltage stability monitoring, assessment, and control using synchrophasor data.

LUIGI VANFRETTI (SM'14) received the M.Sc. and Ph.D. degrees in electric power engineering from the Rensselaer Polytechnic Institute, Troy, NY, USA, in 2007 and 2009, respectively. He was with the KTH Royal Institute of Technology, Stockholm, Sweden, as an Assistant, from 2010 to 2013, and as an Associate Professor (Tenured) and a Docent from 2013 to 2017, where he led the SmarTS Lab and the Research Group. He was with the Statnett SF, the Norwegian Electric Power Transmission System Operator, as a Consultant, from 2011 to 2012, and as a Special Advisor in research and development from 2013 to 2016. He joined the Rensselaer Polytechnic Institute in 2017, where he is currently a Tenured Associate Professor. His research interests are in the area of sycnhrophasor technology applications, cyber-physical power system modeling, simulation, stability, and control.